

Investigating the excitation function of HBT radii for Lévy-stable sources

Máté Csanád^a, Dániel Kincses^a

^aELTE Eötvös Loránd University, Pázmány Péter sétány 1/A, Budapest, 1117, Hungary

Abstract

One of the main goals of today's heavy-ion physics research is to explore the phase diagram of strongly interacting matter and search for signs of the possible critical endpoint on the QCD phase diagram. Femtoscopy is among the important tools used for this endeavor; there have been indications that combinations of femtoscopic radii parameters (referred to as HBT radii for identical boson pairs) can be related to the system's emission duration. An apparent non-monotonic behavior in their excitation function thus might signal the location of the critical point. In this paper, we show that conclusions drawn from the results obtained with a Gaussian approximation for the pion source shape might be altered if one utilizes a more general Lévy-stable source description. We find that the characteristic size of the pion source function is strongly connected to the shape of the source and its possible power-law behavior. Taking this into account properly changes the observed behavior of the excitation function.

Keywords: femtoscopy, HBT correlations, Lévy-stable distribution, critical point

1. Introduction

Exploring the phase diagram of strongly interacting matter is a cornerstone of heavy-ion physics research [1]. The quest to pinpoint the critical endpoint on the Quantum Chromodynamics (QCD) phase diagram is ongoing, and femtoscopy serves as a pivotal tool in this endeavor [2]. It has been demonstrated that femtoscopic radii parameters (also called HBT radii, after R. Hanbury-Brown and R. Q. Twiss [3]) extracted from two-particle interferometry measurements are sensitive to the emission duration of heavy-ion collisions [4]. In the RHIC Beam Energy Scan program [2], a non-monotonic collision energy (and consequently baryochemical potential) dependence of these parameters was observed [5], which was suggested to be a sign of possible critical behavior [6]. These measurements assumed a Gaussian distribution for the shape of the two-particle emission distribution. Recent results from both experiment [7–11] and phenomenology [12–15] showed that the shape of the pion pair-source follows a Lévy-stable distribution [16] and exhibits a power-law tail. While new measurements in this direction are ongoing, in this paper we describe a method to estimate the effect of the different source shapes on the previous results, based on already published data. In particular, we demonstrate that using a Lévy-stable assumption for the pion pair source can drastically change the trends of the radii parameters as a function of collision energy, and thus the previous conclusions drawn from the Gaussian measurements might need to be reiterated.

1.1. Basic definitions

Utilizing the smoothness approximation [17], where the members of the investigated particle pair have approximately identical momenta, the two-particle correlation function (as a

function of their relative momentum \mathbf{q} and average momentum \mathbf{K}) is defined as

$$C_2(\mathbf{q}, \mathbf{K}) = \int d^3r D(\mathbf{r}, \mathbf{K}) |\psi_{\mathbf{q}}^{(2)}(\mathbf{r})|^2, \quad (1)$$

where $D(\mathbf{r}, \mathbf{K})$ is the pair source distribution (also called spatial correlation function or pair emission function), and $\psi_{\mathbf{q}}^{(2)}(\mathbf{r})$ is the symmetrized pair wave function [18]. Neglecting final-state interactions, the modulus square of the wave function is simply $1 + \cos(\mathbf{q}\mathbf{r})$, thus the correlation function is in direct connection with the Fourier-transform of the spatial correlation function:

$$C_2^{(0)}(\mathbf{q}, \mathbf{K}) \approx 1 + \tilde{D}(\mathbf{q}, \mathbf{K}), \quad (2)$$

where the ⁽⁰⁾ superscript denotes the lack of final-state interactions, and \tilde{D} denotes the Fourier transform of D in its first variable.

If one assumes a shape or functional form for the pair source distribution, one can calculate the shape of the correlation function as well. The dependence on \mathbf{K} is then usually understood to be realized through the parameters of the source, such as its width. Subsequently, one can test the initial assumption via fits to experimentally measured momentum correlation functions. Recent investigations [7–10] showed that assuming a so-called Lévy-stable distribution (a generalization of the Gaussian distribution) for the shape of the source might provide a statistically superior description to the measured two-pion correlation functions.

The three-dimensional symmetric Lévy-stable distribution is

defined as [19]

$$\mathcal{L}(\alpha, \mathbf{R}^2; \mathbf{x}) = \frac{1}{2\pi^3} \int d^3\omega \exp\left(i\omega\mathbf{x} - \frac{1}{2}|\omega^T \mathbf{R}^2 \omega|^{\alpha/2}\right), \quad (3)$$

$$\text{where } \mathbf{R}^2 = \begin{pmatrix} R_o^2 & R_{os}^2 & R_{ol}^2 \\ R_{os}^2 & R_s^2 & R_{sl}^2 \\ R_{ol}^2 & R_{sl}^2 & R_l^2 \end{pmatrix}. \quad (4)$$

Here, \mathbf{R}^2 is a positive definite matrix containing the HBT-radii parameters (also called Lévy-scale parameters), and α is the Lévy exponent. In the above definition of \mathbf{R}^2 we already utilized the usual notation of the Bertsch-Pratt *out – side – long* coordinate system [20, 21], where the *out* direction represents the direction of the average transverse momentum of the particle pair, the *long* direction is the beam direction, and the *side* is perpendicular to both. In the case of an azimuthally integrated experimental analysis, it is usual to neglect the off-diagonal terms, and in the following we will also do this.

Utilizing such a distribution as the pair-source function, in the interaction-free case, the correlation function takes the following form:

$$C_2(q_o, q_s, q_l) = 1 + \lambda \exp\left(-|R_o^2 q_o^2 + R_s^2 q_s^2 + R_l^2 q_l^2|^{\alpha/2}\right). \quad (5)$$

Here, we also introduced the λ correlation strength or intercept parameter [22, 23], that corresponds to the value of the correlation at zero relative momentum (in an interaction-free case). In the case of $\alpha = 2$, the shape of the pair-source and the correlation function is both a Gaussian. In the case of $\alpha < 2$, the pair-source exhibits a power-law behavior, and the correlation function takes the form of a stretched-exponential function. Of course, in the case of an experimental analysis, one needs to properly account for the final-state Coulomb interaction. For Lévy-stable sources, details of such calculations were discussed in Refs. [24–26]; in the following, we use the results presented in Ref. [26].

2. Scaling method

In the first published experimental heavy-ion analysis utilizing a Lévy-stable description for the pion pair source [7], a scaling variable was found, defined as

$$\widehat{R} = \frac{R}{\lambda \cdot (1 + \alpha)}, \quad (6)$$

where R is the one-dimensional Lévy scale parameter.

When fitting the same correlation function with different fixed α values, this parameter seemed remarkably stable. This implies that if we know the λ and R results for a given α assumption, we can deduce the value of these for another α assumption. In particular, if the Gaussian parameters R_G and λ_G (obtained with an assumption of $\alpha = 2$) are known and the $\lambda_{\text{free}\alpha}$ and α values are also known for a free- α fit, then the value of $R_{\text{free}\alpha}$ can be estimated based on

$$\widehat{R}_G \equiv \frac{R_G}{\lambda_G \cdot (1 + 2)} = \widehat{R}_{\text{free}\alpha} \equiv \frac{R_{\text{free}\alpha}}{\lambda_{\text{free}\alpha} \cdot (1 + \alpha)} \quad (7)$$

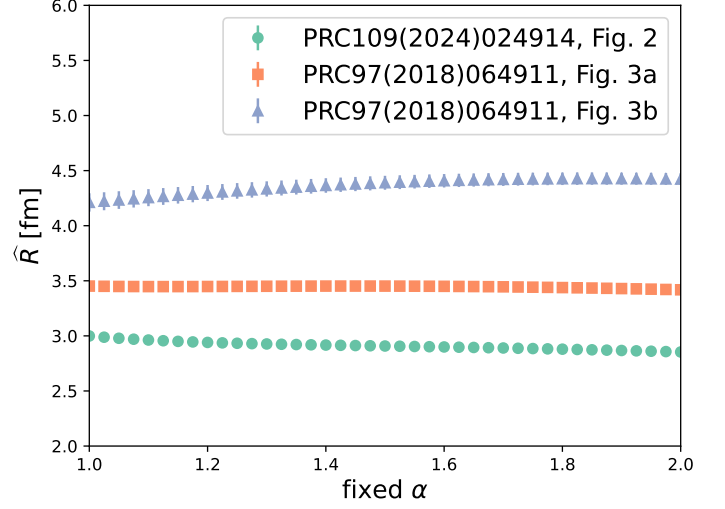


Figure 1: Figure 2 of Ref. [9] and Figs. 3a-3b of Ref. [7]. See detailed parameters in Appendix.

as

$$R_{\text{free}\alpha} = R_G \frac{\lambda_{\text{free}\alpha} \cdot (1 + \alpha)}{\lambda_G \cdot (1 + 2)}. \quad (8)$$

To demonstrate the stability of this scaling variable, we take three example correlation functions from Refs. [7, 9] (from their respective HEPdata entries). Using the correlation function calculation method described in Ref. [26] and the software package given in Ref. [27], we fit these example correlation functions with different fixed α values, with the functional form

$$N \left[1 - \lambda + \lambda(1 + e^{-(qR)^\alpha}) K_C(q; R, \alpha) \right] (1 + \epsilon q), \quad (9)$$

where K_C is the Coulomb correction as calculated in Ref. [26], N is a normalization parameter and ϵ responsible for accounting for any residual, long-range background from non-femtoscopic effects (such as energy and momentum conservation, flow, or minijets). From the resulting fit parameters, we calculate the corresponding $\widehat{R}_{\text{fix}\alpha}$ values. All fit parameters and fit quality indicators are shown in the Appendix. We find that, indeed, in the investigated range, the scaling variable \widehat{R} remains approximately constant as a function of the fixed α value, as demonstrated in Figure 1.

While an experimental confirmation is not yet available, it is natural to assume that this scaling relation also holds for the three-dimensional radii parameters, at least approximately, as a smaller α leads to a more “peaked” correlation function, hence to describe the same data one requires a larger R and a larger λ value. We also assume that the α parameter measured under the assumption of a spherically symmetric source is identical with (or close to) the α obtained from a three-dimensional measurement (which does not assume a spherically symmetric source). Thus we can estimate how the radii would change from the fixed $\alpha = 2$ Gaussian case to the free- α case using published data, as described in the next section.

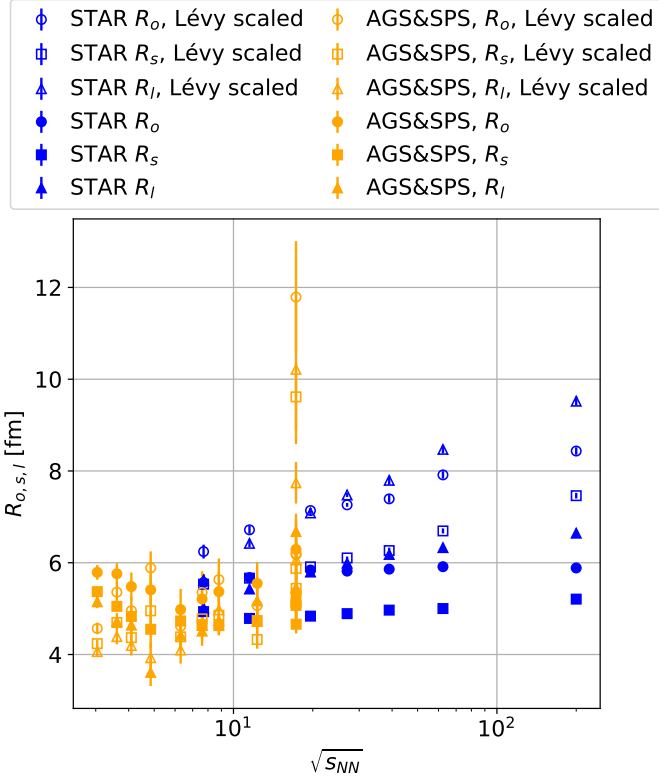


Figure 2: Scaled Lévy parameters $R_{o,s,l}$, compared to the original Gaussian values from Ref. [5]

3. Results and discussion

Measurements based on a Gaussian source assumption were performed in Ref. [5], where also the collision energy dependence of the source parameters (radii and λ) was investigated at $K_T \approx 0.22 \text{ GeV}/c^2$, where K_T is the transverse component of \mathbf{K} . In this paper, a non-monotonic collision energy dependence of $\sqrt{R_{o,G}^2 - R_{s,G}^2}$ was found, as mentioned above.

Based on STAR preliminary results presented at the Zimányi School 2023 and CPOD 2024 conferences¹, one can make a rough approximation of the collision energy dependence of the $\lambda_{\text{free } \alpha}$ and α parameters (also at $K_T \approx 0.22 \text{ GeV}/c^2$) in the form of

$$A_{\text{par}} \left(\frac{\sqrt{s_{NN}}}{E_0} \right)^{B_{\text{par}}}, \quad (10)$$

with

$$A_\alpha = 1.85, B_\alpha = -0.06, A_\lambda = 0.6, B_\lambda = 0.06, \quad (11)$$

¹See talk slides at indico.cern.ch/event/1352455/contributions/5696657/ and conferences.lbl.gov/event/1376/contributions/8829/

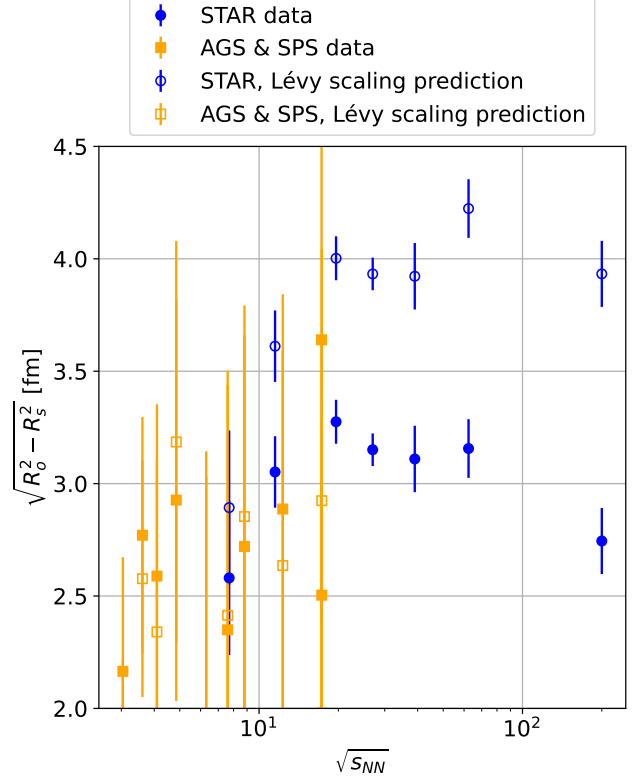


Figure 3: Scaled Lévy parameter difference $\sqrt{R_o^2 - R_s^2}$, compared to the original Gaussian values from Ref. [5]

and $E_0 = 1 \text{ GeV}$ is introduced to remove the unit of $\sqrt{s_{NN}}$. The Gaussian measurements for $R_{G(o,s,l)}$ together with the corresponding λ_G values are available from Ref. [5]. Using these inputs, we calculated the corresponding $R_{\text{free } \alpha(o,s,l)}$ values, as shown in Figure 2. The $\sqrt{R_o^2 - R_s^2}$ difference is shown in Figure 3.

In line with the expected scaling behavior, the smaller α values increase the radii for the Lévy scaling predictions, and with this, the *out* and *side* difference also increases. However, it is interesting to note that the non-monotonic energy dependence is weakened, and the *out* – *side* difference appears to be constant above $\sqrt{s_{NN}} = 19 \text{ GeV}$. These observations demonstrate the need for the three-dimensional HBT measurements utilizing Lévy-stable source distributions.

4. Summary and conclusions

We demonstrated based on three example correlation functions that the variable combination called \hat{R} is indeed a scaling variable, i.e., it does not strongly depend on the assumed α value. We used this scaling relation to infer HBT radii in the out-side-long system with a free α value from results with a Gaussian assumption ($\alpha = 2$). Finally, we investigated the out-side difference as a proxy for emission duration. Our results

indicate that the trend of this difference is strongly affected by the assumption for the shape, and unlike the case of a Gaussian assumption, there may be no non-monotonic behavior of the out-side difference as a function of collision energy. This underlines the importance of performing experimental measurements with an unrestricted α parameter.

Acknowledgements

This research was funded by the NKFIH grants TKP2021-NKTA-64, PD-146589 and K-146913.

References

- [1] P. Achenbach, et al., The present and future of QCD, Nucl. Phys. A 1047 (2024) 122874. arXiv:2303.02579, doi:10.1016/j.nuclphysa.2024.122874.
- [2] A. Bzdak, S. Esumi, V. Koch, J. Liao, M. Stephanov, N. Xu, Mapping the Phases of Quantum Chromodynamics with Beam Energy Scan, Phys. Rept. 853 (2020) 1–87. arXiv:1906.00936, doi:10.1016/j.physrep.2020.01.005.
- [3] R. Hanbury Brown, R. C. Jennison, D. G. M. K., Apparent Angular Sizes of Discrete Radio Sources: Observations at Jodrell Bank, Manchester, Nature 170 (1952) 1061–1063. doi:10.1038/1701061a0.
- [4] S. Chapman, P. Scotto, U. W. Heinz, A New cross term in the two particle HBT correlation function, Phys. Rev. Lett. 74 (1995) 4400–4403. arXiv:hep-ph/9408207, doi:10.1103/PhysRevLett.74.4400.
- [5] L. Adamczyk, et al., Beam-energy-dependent two-pion interferometry and the freeze-out eccentricity of pions measured in heavy ion collisions at the STAR detector, Phys. Rev. C 92 (1) (2015) 014904. arXiv:1403.4972, doi:10.1103/PhysRevC.92.014904.
- [6] R. A. Lacey, Indications for a Critical End Point in the Phase Diagram for Hot and Dense Nuclear Matter, Phys. Rev. Lett. 114 (14) (2015) 142301. arXiv:1411.7931, doi:10.1103/PhysRevLett.114.142301.
- [7] A. Adare, et al., Lévy-stable two-pion Bose-Einstein correlations in $\sqrt{s_{NN}} = 200$ GeV Au+Au collisions at STAR, Phys. Rev. C 97 (6) (2018) 064911, [Erratum: Phys.Rev.C 108, 049905 (2023)]. arXiv:1709.05649, doi:10.1103/PhysRevC.97.064911.
- [8] D. Kincses, Pion Interferometry with Lévy-Stable Sources in $\sqrt{s_{NN}} = 200$ GeV Au + Au Collisions at STAR, Universe 10 (3) (2024) 102. arXiv:2401.11169, doi:10.3390/universe10030102.
- [9] A. Tumasyan, et al., Two-particle Bose-Einstein correlations and their Lévy parameters in PbPb collisions at $\sqrt{s_{NN}}=5.02$ TeV, Phys. Rev. C 109 (2) (2024) 024914. arXiv:2306.11574, doi:10.1103/PhysRevC.109.024914.
- [10] H. Adhikary, et al., Two-pion femtoscopic correlations in Be+Be collisions at $\sqrt{s_{NN}} = 16.84$ GeV measured by the NA61/SHINE at CERN, Eur. Phys. J. C 83 (10) (2023) 919. arXiv:2302.04593, doi:10.1140/epjc/s10052-023-11997-8.
- [11] B. Porfy, Femtoscopy at NA61/SHINE using symmetric Lévy sources in central $^{40}\text{Ar}+^{45}\text{Sc}$ from 40A GeV/c to 150A GeV/c, 2024. arXiv:2406.02242.
- [12] B. Kórodi, D. Kincses, M. Csanád, Event-by-event investigation of the two-particle source function in $\sqrt{s_{NN}}=2.76$ TeV PbPb collisions with EPOS, Phys. Lett. B 847 (2023) 138295. arXiv:2212.02980, doi:10.1016/j.physletb.2023.138295.
- [13] D. Kincses, M. Stefaniak, M. Csanád, Event-by-Event Investigation of the Two-Particle Source Function in Heavy-Ion Collisions with EPOS, Entropy 24 (3) (2022) 308. arXiv:2201.07962, doi:10.3390/e24030308.
- [14] A. Ayala, S. Bernal-Langarica, I. Dominguez, I. Maldonado, M. E. Tejeda-Yeomans, Collision energy dependence of source sizes for primary and secondary pions at NICA energies (12 2023). arXiv:2401.00619.
- [15] M. Csanád, D. Kincses, Femtoscopy with Lévy Sources from SPS through RHIC to LHC, Universe 10 (2) (2024) 54. arXiv:2401.01249, doi:10.3390/universe10020054.
- [16] Csörgő, T. and Hegyi, S. and Zajc, W. A., Bose-Einstein correlations for Lévy stable source distributions, Eur. Phys. J. C 36 (2004) 67–78. arXiv:nucl-th/0310042, doi:10.1140/epjc/s2004-01870-9.
- [17] S. Pratt, Validity of the smoothness assumption for calculating two-boson correlations in high-energy collisions, Phys. Rev. C 56 (1997) 1095–1098. doi:10.1103/PhysRevC.56.1095.
- [18] M. A. Lisa, S. Pratt, R. Soltz, U. Wiedemann, Femtoscopy in relativistic heavy ion collisions, Ann. Rev. Nucl. Part. Sci. 55 (2005) 357–402. arXiv:nucl-ex/0505014, doi:10.1146/annurev.nucl.55.090704.151533.
- [19] J. P. Nolan, Financial modeling with heavy-tailed stable distributions, WIREs Computational Statistics 6 (1) (2014) 45–55. arXiv:https://wires.onlinelibrary.wiley.com/doi/pdf/10.1002/wics.1286, doi:https://doi.org/10.1002/wics.1286. URL https://wires.onlinelibrary.wiley.com/doi/abs/10.1002/wics.1286
- [20] G. Bertsch, M. Gong, M. Tohyama, Pion Interferometry in Ultrarelativistic Heavy Ion Collisions, Phys. Rev. C 37 (1988) 1896–1900. doi:10.1103/PhysRevC.37.1896.
- [21] S. Pratt, T. Csorgo, J. Zimanyi, Detailed predictions for two pion correlations in ultrarelativistic heavy ion collisions, Phys. Rev. C 42 (1990) 2646–2652. doi:10.1103/PhysRevC.42.2646.
- [22] Csörgő, T. and Lörstad, B. and Zimányi, J., Bose-Einstein correlations for systems with large halo, Z. Phys. C 71 (1996) 491–497. arXiv:hep-ph/9411307, doi:10.1007/s002880050195.
- [23] J. Bolz, U. Ornik, M. Plumer, B. R. Schlei, R. M. Weiner, Resonance decays and partial coherence in Bose-Einstein correlations, Phys. Rev. D 47 (1993) 3860–3870. doi:10.1103/PhysRevD.47.3860.
- [24] D. Kincses, M. I. Nagy, M. Csanád, Coulomb and strong interactions in the final state of Hanbury-Brown–Twiss correlations for Lévy-type source functions, Phys. Rev. C 102 (6) (2020) 064912. arXiv:1912.01381, doi:10.1103/PhysRevC.102.064912.
- [25] M. Csanád, S. Lökös, M. Nagy, Expanded empirical formula for Coulomb final state interaction in the presence of Lévy sources, Phys. Part. Nucl. 51 (3) (2020) 238–242. arXiv:1910.02231, doi:10.1134/S1063779620030089.
- [26] M. Nagy, A. Purzsa, M. Csanád, D. Kincses, A novel method for calculating Bose–Einstein correlation functions with Coulomb final-state interaction, Eur. Phys. J. C 83 (11) (2023) 1015. arXiv:2308.10745, doi:10.1140/epjc/s10052-023-12161-y.
- [27] Correlation function calculation with Lévy source and Coulomb FSI (2023). URL https://https://github.com/csanadm/CoulCorrLevyIntegral
- [28] F. James, M. Roos, Minuit: A system for function minimization and analysis of the parameter errors and correlations, Comput. Phys. Commun. 10 (1975) 343–367. doi:10.1016/0010-4655(75)90039-9.

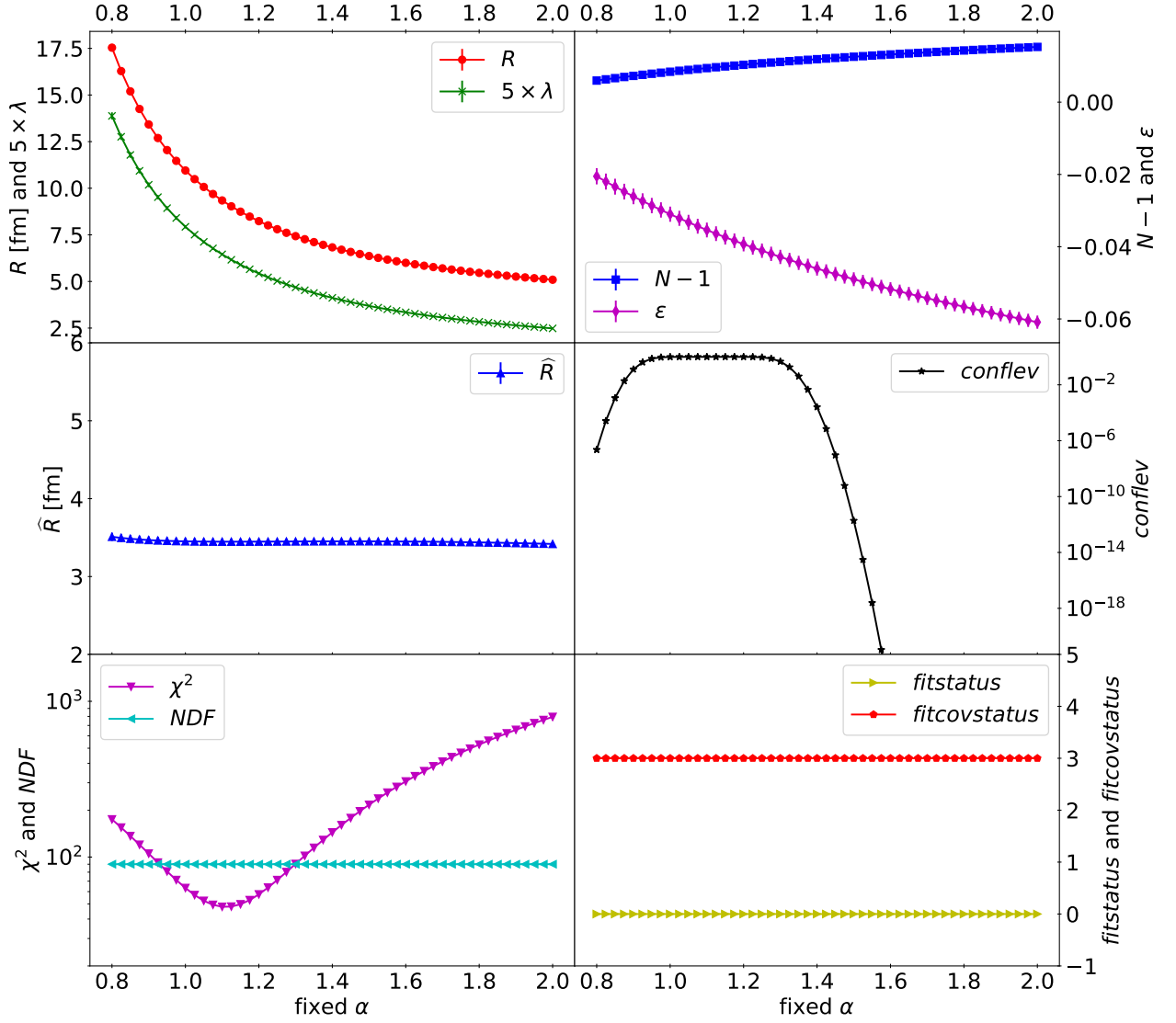


Figure 4: Fit parameters and quality from various fixed- α fits to correlation function data of Figure 3a from Ref. [7]. The plots show parameters R and λ , fit normalization parameter N and residual slope ϵ , scaling parameter \widehat{R} , confidence level, χ^2 and NDF, as well as the “fit status” and “covariance matrix status” parameters.

Appendix A

Figs. 4, 5, and 6 show all fit parameters (R , λ , N , ϵ) and fit quality indicators (χ^2 , NDF, confidence level, fit status and covariance matrix status), along with the scaling variable \widehat{R} , for many cases of fixed α values from 0.8 to 2.0. Here NDF means the number of degrees of freedom (number of data points minus the number of free fit parameters), confidence level means the p-value of the fit (calculated from χ^2 and NDF), fit status and covariance matrix status come from the Minuit optimization library [28], and their best values are 0 and 3, respectively (indicating a fully converged fit and fully positive definite covariance matrix). These fit quality indicators are important as they demonstrate the good quality of the fits. Without them, one cannot be sure that the best fit parameters indeed do represent the data. These plots show that (especially for larger α , above ~ 1.4) the scaling variable \widehat{R} is indeed independent of the assumed fix α value, hence can be used to infer R at a given α from R at a different α .

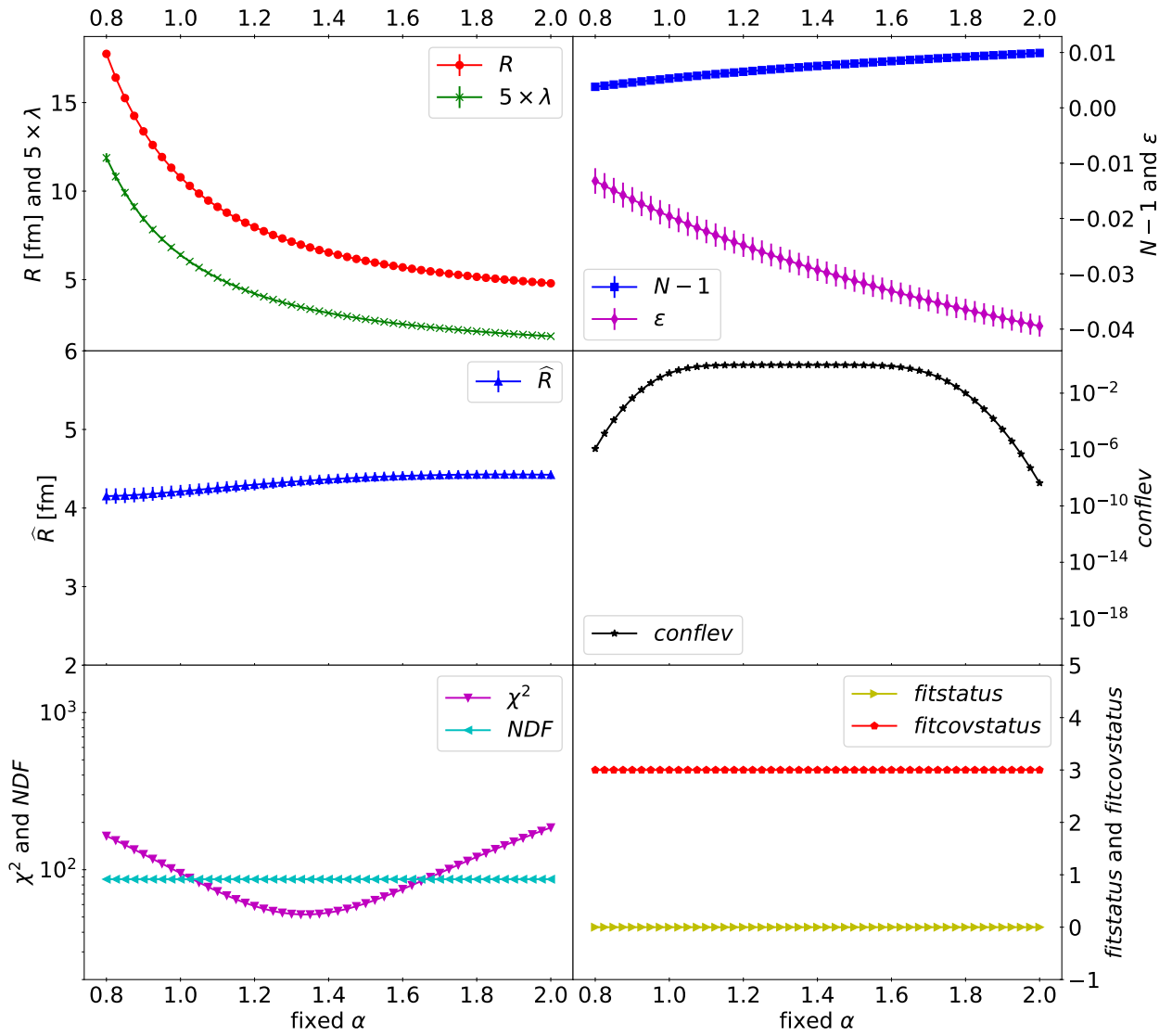


Figure 5: Fit parameters and quality from various fixed- α fits to correlation function data of Figure 3b from Ref. [7], similarly to Fig. 4.

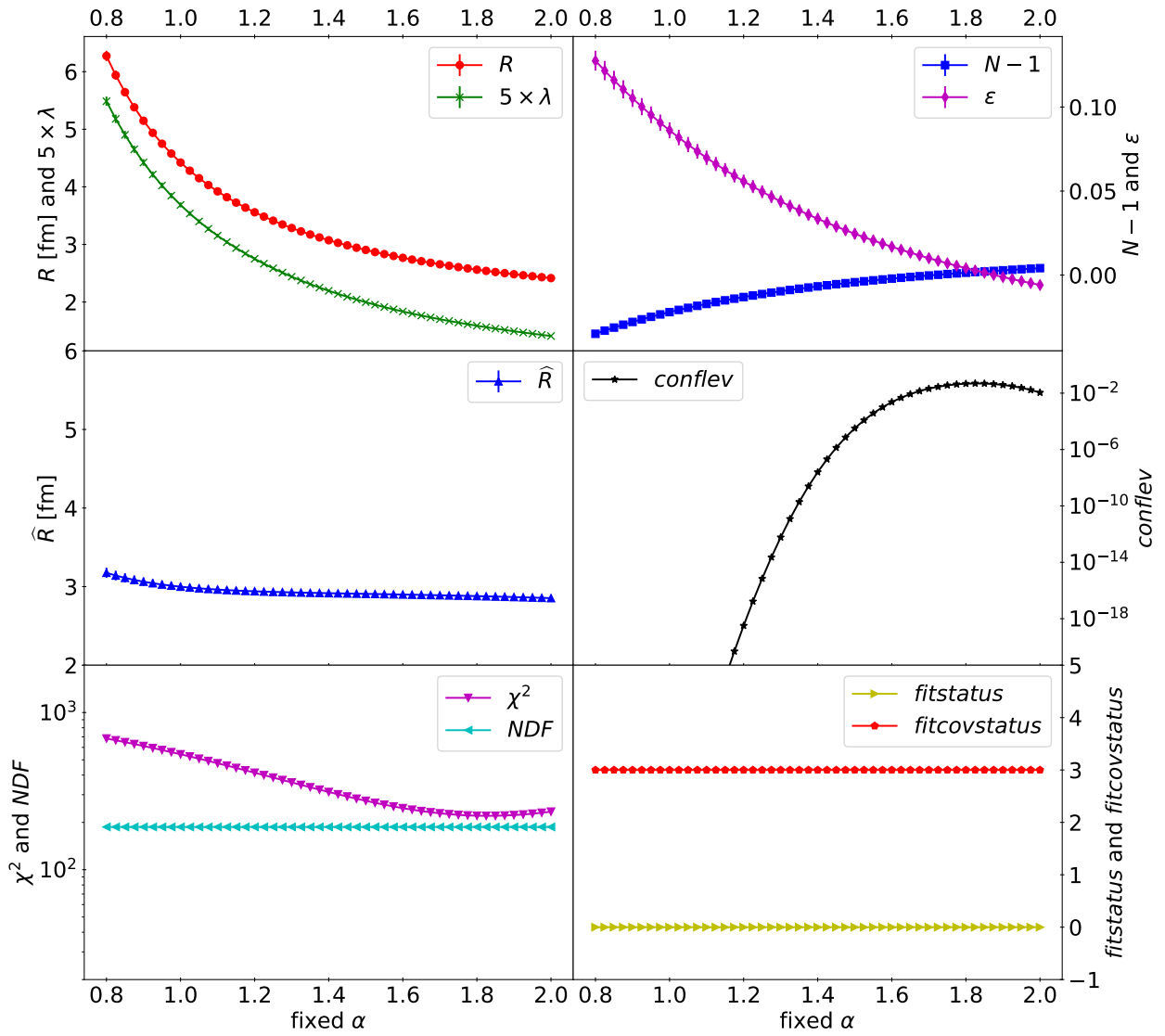


Figure 6: Fit parameters and quality from various fixed- α fits to correlation function data of Figure 2 from Ref. [9], similarly to Fig. 4.